Image-inpainting and quality-guided phase unwrapping algorithm

AUTHOR(S):

Meng, Lei; Fang, Suping; Yang, Pengcheng; Wang, Leijie; Komori, Masaharu; Kubo, Aizoh

CITATION:

Meng, Lei ...[et al]. Image-inpainting and quality-guided phase unwrapping algorithm. Applied Optics 2012, 51(13): 2457-2462

ISSUE DATE:

2012-05-01

URL:

http://hdl.handle.net/2433/193731

Image-inpainting and quality-guided phase unwrapping algorithm

Lei Meng,[1] Suping Fang,[1,*] Pengcheng Yang,[1] Leijie Wang,[1] Masaharu Komori,[2] and Aizoh Kubo[2]

[1]State Key Laboratory for Manufacturing Systems Engineering, Xi'an Jiaotong University, Xi'an 710049, China

[2]Department of Precision Engineering, Faculty of Engineering, Kyoto University, Yoshida Honmachi, Sakkyo-ku, Kyoto 606-8501, Japan

*Corresponding author: spfang@mail.xjtu.edu.cn

Received 9 December 2011; revised 6 February 2012; accepted 10 February 2012; posted 13 February 2012 (Doc. ID 159753); published 1 May 2012

For the wrapped phase map with regional abnormal fringes, a new phase unwrapping algorithm that combines the image-inpainting theory and the quality-guided phase unwrapping algorithm is proposed. First, by applying a threshold to the modulation map, the valid region (i.e., the interference region) is divided into the doubtful region (called the target region during the inpainting period) and the reasonable one (the source region). The wrapped phase of the doubtful region is thought to be unreliable, and the data are abandoned temporarily. Using the region-filling image-inpainting method, the blank target region is filled with new data, while nothing is changed in the source region. A new wrapped phase map is generated, and then it is unwrapped with the quality-guided phase unwrapping algorithm. Finally, a postprocessing operation is proposed for the final result. Experimental results have shown that the performance of the proposed algorithm is effective. © 2012 Optical Society of America

OCIS codes: 100.5070, 100.5088, 120.3180.

1. Introduction

Phase unwrapping is a key technique in optical interferometry, synthetic aperture radar (SAR), and magnetic resonance imaging [1]. Many new and promising algorithms have been presented in past decades. As discussed by Aebischer and Waldner [2] and Qian *et al.* [3], the problem of phase unwrapping can be studied from two extreme perspectives. In the first point of view, all efforts are concentrated on the unwrapping algorithm, and there is no special algorithm for filtering. At present, most phase unwrapping algorithms [4–9] follow this method. However, without filtering, phase unwrapping becomes inconceivably difficult. If the integration path runs through or around pixels with problematic phase, it is hard to assure the accuracy of the unwrapped result. In the latter case, all efforts are put into improving the filtering algorithm to get a wrapped phase map with sufficiently high quality, and the unwrapping process becomes trivial. Recently, many new filtering algorithms [2,10–13] have been proposed. Most of them perform rather well on the phase map with severe random noise. However, they almost fail while coping with phase maps obtained by our laser interferometer for measurement of tooth flanks of involute helical gears [14–17]. The tooth surface is a continuous surface, but its roughness is far larger than that of optical elements, resulting in a wrapped phase map with regional abnormal fringes. In that situation, filtering seems unhelpful. For example, Fig. 1(a) is part of a practical wrapped phase map. The fringes in regions R and S are mismatched or blurred heavily. Figure 1(b) shows the result filtered by the windowed Fourier transform approach [2,12]. Apparently, most random noise has been effectively removed, but the problems in regions R and S

1559-128X/12/132457-06$15.00/0

remain. Mismatched fringes have not been corrected. No high-quality wrapped phase map is obtained, and the following unwrapping process is no longer trivial. Figures 1(c) and 1(d) show the unwrapped results of the two wrapped phase maps using the quality-guided (QG) phase unwrapping algorithm [1,3]. Luckily, the QG phase unwrapping algorithm successfully overcomes the problem in region R, and both unwrapped results there are acceptable. However, both maps have a failure at the lower left corner. (With reference to the unwrapped result using our proposed algorithm in the experiment section, it is easier to reach such a conclusion.) Both the direct unwrapping method and the filtering method are dissatisfactory while coping with phase maps with regional abnormal fringes.

To address the issue, this paper presents an image-inpainting (II) and QG phase unwrapping algorithm. An II process is needed before the true unwrapping process. The preprocessing operation only works on a small part of the wrapped phase map, and the other region has no change to its wrapped phase value. The region needing preprocessing is called the doubt region (the target region), and the other is called the reasonable region (the source region). The preprocessing operation is performed in two steps: defining the target region and filling it with data extracted from the source region. As a result, the phase of the doubtful region is replicated by the good phase from the reasonable region. A new wrapped phase map with high quality is generated, and the unwrapping process becomes trivial.

The principle of the proposed algorithm is elaborated upon in Section 2. In Section 3, two experiments that have been performed are described. Conclusions are presented in Section 4.

2. Description of the Algorithm

The proposed algorithm consists of four steps: defining the doubtful region, filling the doubtful region, QG phase unwrapping, and postprocessing.

A. Definition of the Doubtful Region

Defining the doubtful region involves identifying the area that covers as many pixels with a problematic phase as possible and as few reasonable pixels as possible.

As far as we know, phase derivative variance (PDV), pseudocorrelation, and maximum phase gradient [1] are the three most common parameters used to define the quality or goodness of each pixel of the given phase data. Moreover, correlation in SAR [1] and modulation in the phase-shifting interferometry [18] can also be used as the reliability measure. The first three parameters are a direct reflection of the wrapped phase and more suitable to guide the unwrapping path. The latter two are counterparts of the wrapped phase data, and they can be used to define whether the practical wrapped phase of each pixel is reasonable [9]. Both experiments in this paper were performed on a phase-shifting

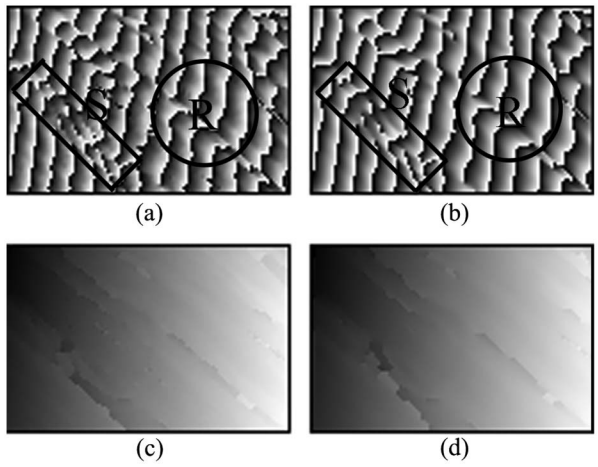

Fig. 1. Problem of the filtering method: (a) original wrapped phase map (105 × 69 pixels), (b) after filtering (the window size $\sigma = 3$), (c) unwrapped result of the original wrapped phase, and (d) unwrapped result of the filtered wrapped phase map.

interferometer [14–17]. Hence, modulation is used to distinguish the doubtful region from the reasonable region. Modulation is derived as follows [18]:

$$M(x,y) = \frac{2}{N}\left[\left(\sum_{k=0}^{N-1} I_k(x,y)\cos(2\pi k/N)\right)^2 + \left(\sum_{k=0}^{N-1} I_k(x,y)\sin(2\pi k/N)\right)^2\right]^{1/2}, \quad (1)$$

where (x,y) represents the coordinate value, N is the total number of the phase-shifting steps, and $I_k(x,y)$ is the intensity distribution of the kth interferogram. For convenience, the modulation value is stretched to the interval [0, 255] and shown in a gray-level image.

By applying a threshold to the modulation map, we can separate the valid region into the reasonable region and the doubtful region easily. All pixels with modulation values below the threshold are defined to be doubtful, and those above or equal to the threshold are reasonable. The main difficulty is the selection of the threshold [1]. If the threshold is too low, too many problematic pixels are left, and the inpainting process will be affected badly. If the threshold is too high, too many reasonable pixels are masked out, and there is not enough exemplar information for the inpainting process.

The threshold is usually chosen manually by a human operator, but it is not suitable for automatic processing. An automated method to select the threshold is proposed by Ghiglia and Pritt [1], and it can be applied to this paper with a minor change. The threshold defined by the automated method is relatively low for the purpose of preventing large regions from isolating from each other. However, in this paper, there is no such special requirement. Hence, there should be a relaxation to the original threshold. The change is as follows:

$$T_n = \alpha T_o, \tag{2}$$

where T_n is the new threshold, T_o represents the original threshold chosen by the automated method, and α is the relaxation parameter. According to our experiments, α is proposed to be 1.2–1.3, and the default value is 1.2.

B. Filling the Target Region

Once the target region is defined, the next step is to fill it. At present, the II technique can be classified into two categories: the partial differential equation-based algorithm [19–21] and the exemplar-based (EB) one [22–25]. The former method is more suitable for images needing small-scale restoration. The latter one performs well on images with textures, and it can even competently accomplish the restoration of images with large-scale damage [25]. The fringe of the wrapped phase map is a kind of texture. Hence, the EB method is preferred. Many EB algorithms have been presented, and the region-filling algorithm is one of the most successful algorithms. Detailed descriptions are available as well [24,25]. A brief introduction is shown in Fig. 2 as follows.

(1) Select the target region Ω. The other place of the valid region is called the source region Φ.

(2) Specify the size of the template window Ψ. A default size of 9×9 pixels is proposed.

(3) Calculate the patch priority $P(p)$. Given a contour patch Ψ_p centered at the point p, its priority $P(p)$ is defined as follows:

$$P(p) = C(p).D(p), \tag{3}$$

where $C(p)$ is called the confidence term and $D(p)$ the data term. $C(p)$ is used to measure the amount of reliable information around the pixel p. It is defined as follows:

$$C(p) = \frac{\sum_{s \in \Psi_p \cap \Phi} C(s)}{|\Psi_p|}, \tag{4}$$

where $|\Psi_p|$ is the area of Ψ_p. During initialization, the function $C(p)$ is set to $C(p) = 0 \forall p \in \Omega$ and $C(p) = 1 \forall p \in \Phi$. $D(p)$ is an indicator of the strength of isophotes hitting the contour $\delta\Omega$ at each iteration. It can be calculated as follows:

$$D(p) = \frac{|\nabla I_p^{\perp}.n_p|}{a}, \tag{5}$$

where $\nabla I_p^{\perp}$ is the isophote (direction and intensity) at point p, n_p is the normal to the contour $\delta\Omega$, and a is a normalization factor. Once all priorities on the contour $\delta\Omega$ have been computed, the patch $\Psi_{\hat{p}}$ with the highest priority is found, and the next step is to fill it with data from the source region Φ.

(4) Search for the most similar patch $\Psi_{\hat{q}}$. Before the filling process, it is necessary to define which patch is most similar to $\Psi_{\hat{p}}$. Formally, the patch $\Psi_{\hat{q}}$ is thought to be the most similar one if the following requirement is fulfilled:

$$\Psi_{\hat{q}} = \arg \min_{\Psi_q \in \Phi} \mathrm{dist}(\Psi_{\hat{p}}, \Psi_q), \tag{6}$$

where $\mathrm{dist}(\Psi_{\hat{p}}, \Psi_q)$ is simply defined as the sum of squared differences (SSD) of the already-filled pixels in the two patches.

(5) Fill the highest-priority patch $\Psi_{\hat{p}}$. Each target pixel in the patch $\Psi_{\hat{p}}$ is filled with the data from the corresponding pixel of the source exemplar $\Psi_{\hat{q}}$, and its confidence is updated as follows:

$$C(t) = C(\hat{p}) \forall\, t \in \Psi_{\hat{p}} \cap \Omega. \tag{7}$$

After the filling process, each pixel of the patch $\Psi_{\hat{p}}$ no longer belongs to the target region. It is treated as the source pixel during the following inpainting process.

(6) The previous three steps [(3), (4), and (5)] will go on iteratively until all target pixels are filled.

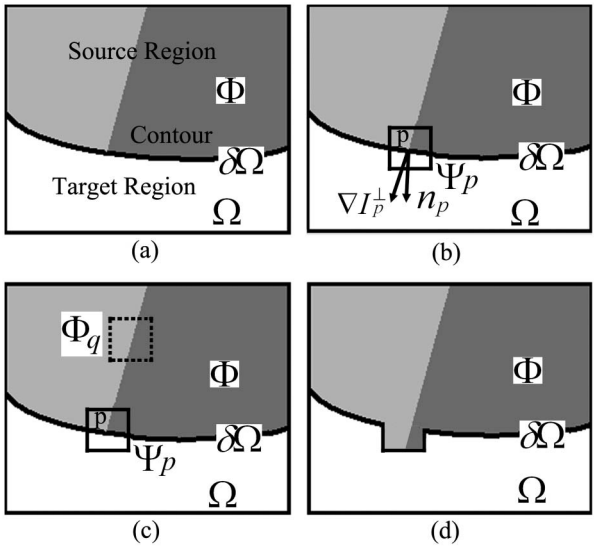

Fig. 2. Structure propagation of RF algorithm: (a) original image with the target region Ω, the contour $\delta\Omega$, and the source region Φ; (b) patch Ψ_p centered at point p ($p \in \delta\Omega$); (c) most likely candidate Ψ_q; (d) partial filling of Ψ_p. Only the target pixel in the patch Ψ_p is filled with the value of the corresponding pixel in Ψ_q.

C. QG Phase Unwrapping

After restoration, a new wrapped phase map is generated. It is unwrapped with the QG path-following phase unwrapping algorithm using PDV as the quality map. The QG path-following phase unwrapping algorithm is a standard procedure that has been previously described [1,3] and will therefore not be discussed here.

D. Postprocessing

Because of inpainting, the wrapped phase in the target region is changed. The following unwrapping process is based on the new phase data. Hence, the unwrapped result of each pixel in the target region has little to do with the original wrapped phase. There may be different requirements for the ultimate unwrapped phase map, and a postprocessing operation

is proposed. It mainly includes two categories: the congruence operation and the continuity operation.

1. Congruence Operation

Congruence means that the difference of each pixel between the unwrapped phase value and the original wrapped phase value is the integer of 2π. In most cases, what is needed is an unwrapped phase map that is congruent everywhere. The simplest way for the congruence operation is as follows:

$$\phi^u(x,y) = \varphi(x,y) + \mathrm{int}\left(\frac{\phi^r(x,y) - \varphi(x,y)}{2\pi}\right)2\pi, \quad (8)$$

where $\phi^u(x,y)$ represents the result after the congruence operation, $\varphi(x,y)$ means the original wrapped phase, $\phi^r(x,y)$ is the unwrapped result of the restored wrapped phase map, and $\mathrm{int}(x)$ stands for the integer closest to x. After the congruence operation, it is certain that the new phase map is congruent with the original wrapped phase map everywhere.

2. Continuity Operation

In special cases, the aim is to reach a continuous map. In that situation, the change of phase data caused by inpainting does not seem to be that important. The result would be acceptable if no distortion and error appear in a large area. The inpainting operation only works on the target region, and the new phase data there can be thought of as the interpolation values to smooth these bad regions. However, the inpainting process is actually a kind of data copy and transplant. It is inevitable that a minority of the patch boundaries is unnatural, and discontinuity may emerge there. (Discontinuity means the difference of the phase values between two adjacent pixels is larger than π.) Some special operation is needed to remove these discontinuous pixels. In our experience, the simple two-dimensional median filtering is well enough to do that job. The 3×3 neighborhood is often used as the default window, but a 5×5 pixel window is more effective in our experience.

3. Experiment Verification

The first example is related to Fig. 1. It consists of Figs. 3 and 4. Figure 3(a) shows the modulation map. By the automated method, the original threshold T_o is chosen to be 51. After relaxation, the new threshold T_n is 61. The doubtful region (the target region) defined by 61 is shown in dark in Fig. 3(b). Figure 3(c) shows the restored result. Obviously, the fringes in R and S are corrected hugely. Compared with Fig. 1(a), the texture of the new wrapped phase map becomes clearer, and the unwrapping becomes easier. Of course, there are still some flaws. Something is still wrong with the new fringes in region S, but the bad affection has been greatly reduced. Figure 3(d) shows the unwrapped result of the restored wrapped phase map using the QG algorithm. Visually, no error occurs in a large area, and the result is acceptable. Figure 3(e) is the result of the

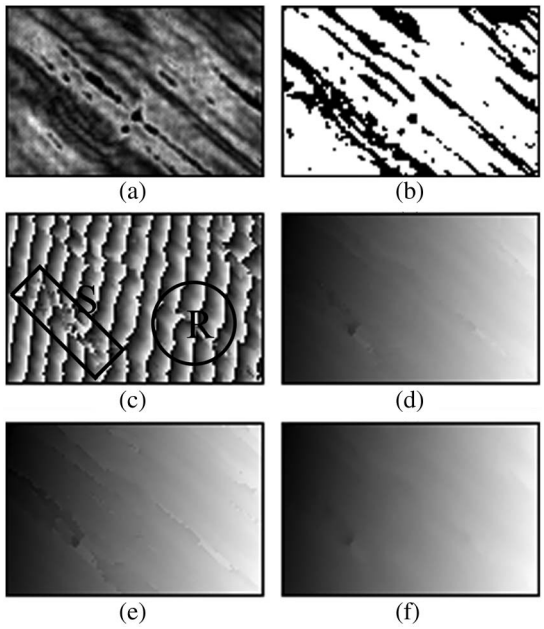

Fig. 3. (a) Modulation map, (b) source region (white pixels) and target region (dark pixels), (c) restored wrapped phase map, (d) unwrapped result of the restored phase data using the quality-guided algorithm, (e) after the congruence operation, and (f) after the continuity operation.

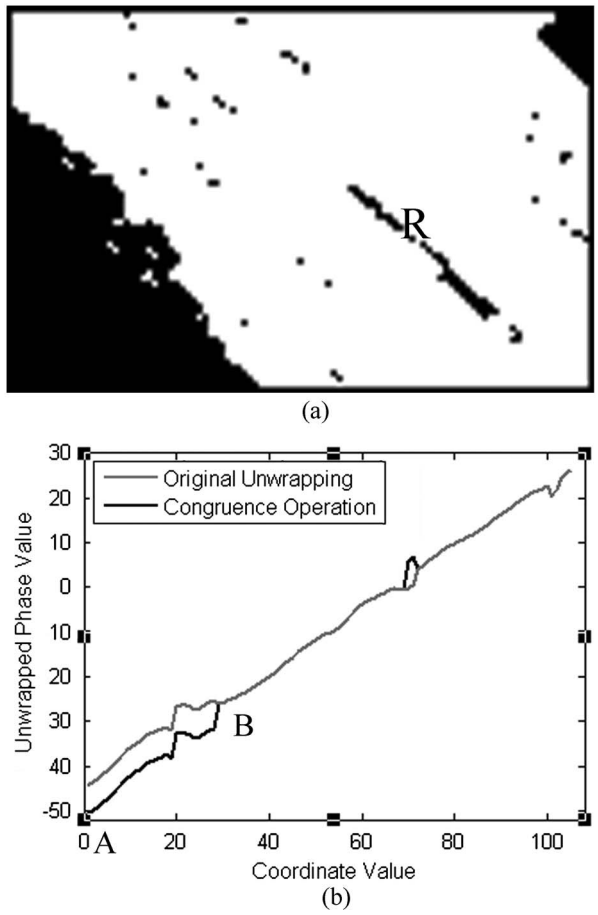

Fig. 4. Comparison between Fig. 1(c) and Fig. 3(e): (a) error map, (b) diagram generated with the 40th row phase data.

congruence operation. After the congruence operation, the new phase data in Fig. 3(e) are congruent with the original wrapped phase data. Figure 1(c) is the unwrapped result of the original wrapped phase. It is also congruent. The comparison between the two maps is shown in Fig. 4. Figure 4(a) shows the error map, where the dark pixels represent discrepancies between the two maps. Obviously, the two results have differences at the lower left corner and the upper right corner. Visually, Fig. 3(e) is more reasonable in both regions. A more convincing and simple way is shown in Fig. 4(b). By extracting phase data from the 40th row of both unwrapped results, a diagram is generated. The gray line has a general rise on the AB segment, causing an error of 2π. In comparison, the dark one is more rational, and the result of the congruence operation is more reasonable. (Using fingers to keep the B point makes it is easier to judge which curve is more feasible.) In Fig. 4(a), there are still many tiny black regions because these regions have ambiguous phase data. For example, the fringes in region R are heavily mismatched. It is difficult and even impossible to pinpoint the most appropriate "cut line" of these mismatched fringes, even in a manual manner. Hence, we believe these differences in such tiny regions are tolerable. Figure 3(f) is the result of the continuity operation. Compared with Fig. 3(d), the filtered result is more smooth and natural.

The other example is shown in Figs. 5–7. Compared with the first one, the second is much more complicated. The lower left corner is an invalid region, and no operation is performed there. As shown in Fig. 5(a), the fringes in regions R, S, T, and U are heavily mismatched, and the texture is not that clear. After inpainting, few fringes are left with mismatch, and the texture is clearer at a glance. Figure 6 shows the unwrapped results. The dark pixel in these maps indicates that the unwrapped surface there is discontinuous. Figure 6(a) is the unwrapped result of the original wrapped phase map. There are plenty of pixels with discontinuity. However, with inpainting, the situation is completely different. Figure 6(b) is the unwrapped result of the restored wrapped phase map. Only a few pixels are discontinuous. The unwrapped result has been greatly improved by the inpainting process. Figure 6(c) is the result of the congruence operation. It is similar to Fig. 6(a), but there are still important differences. The greatest discrepancy between the two grayscale phase images is where the discontinuous pixel appears. A systematic comparison between the two results is shown in Fig. 7. Figure 7(a) is the error map. As in the first example, dark pixels mean discrepancies. It is surprising that the two results are the same only in the middle area. For a quantitative comparison, phase data from the 75th row of the results were extracted and the diagram in Fig. 7(b) generated. Obviously, the gray line has errors on both AB and CD segments. In comparison, the dark one is more rational. In conclusion, the result of the congruence operation is more reasonable, and Fig. 6(a) is a failure.

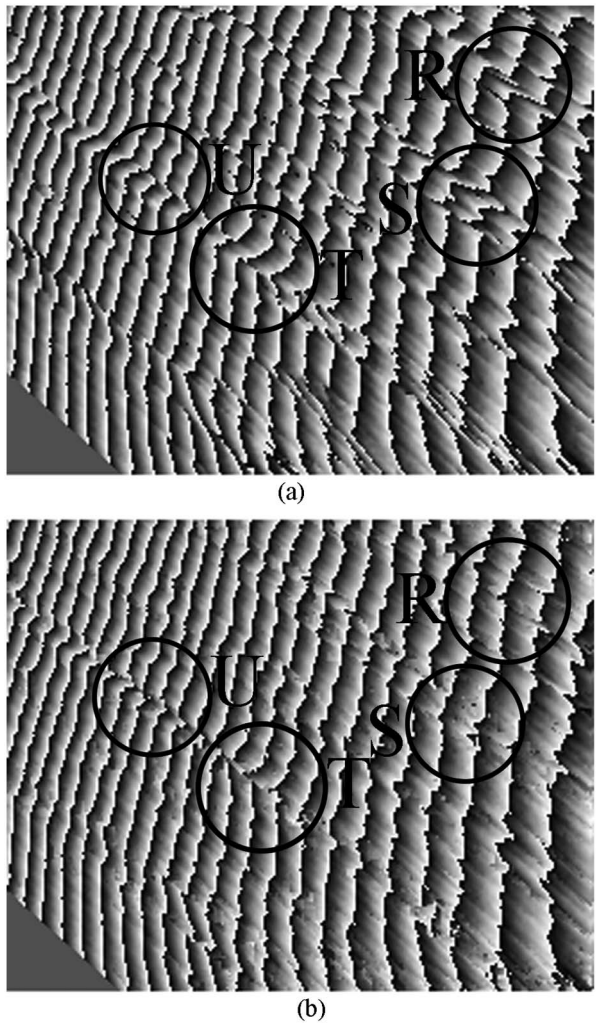

Fig. 5. Wrapped phase maps: (a) original wrapped phase map (250×200 pixels), (b) after inpainting.

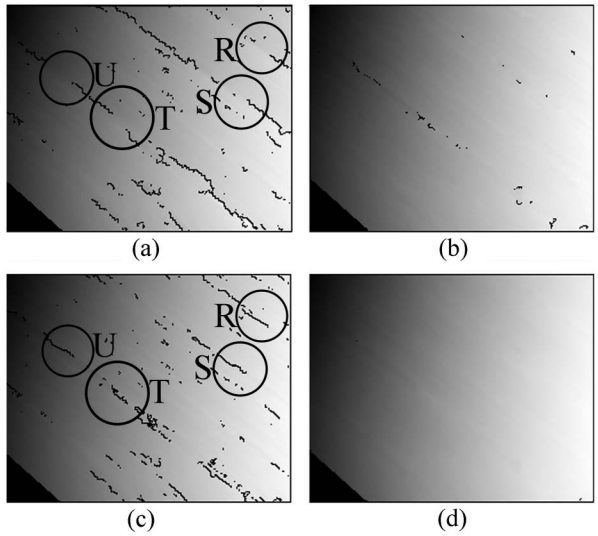

Fig. 6. Unwrapped results: (a) unwrapped result of the original wrapped phase map, (b) unwrapped result of the restored wrapped phase map, (c) after the congruence operation, and (d) after the continuity operation.

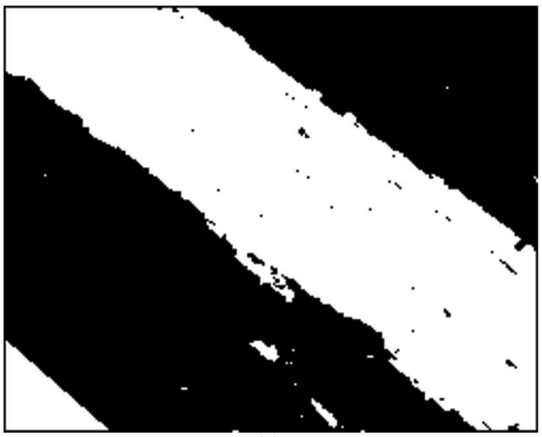

(a)

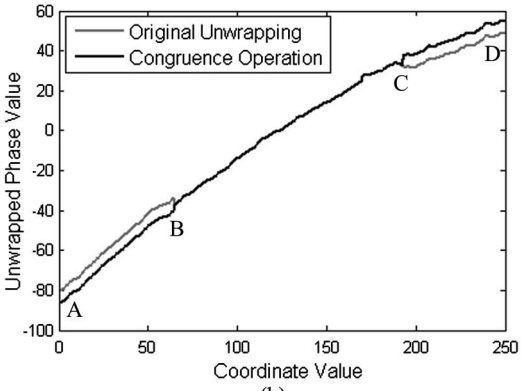

(b)

Fig. 7. Comparison between Figs. 6(a) and 6(c): (a) error map, (b) diagram generated with the 75th row phase data.

Figure 6(d) is the result of the continuity operation. As expected, few pixels are left with discontinuity, and the unwrapped phase map can be seen as a continuous surface.

4. Conclusion

We have developed an II and QG phase unwrapping algorithm for wrapped phase maps with regional abnormal fringes. Using the region-filling II algorithm, we replace these problematic fringes with new data. A new wrapped phase map is generated. Subsequently, it is unwrapped with the QG phase unwrapping algorithm. The unwrapped result is only an interim result. For the ultimate result, we propose a postprocessing operation. Two examples have shown that our method performed well.

Both the region-filling algorithm and the QG algorithm can be reached easily, and the proposed algorithm can be implemented without much effort.

This work was supported by the National Natural Science Foundation of China under grant no. 50875205.

References

1. D. C. Ghiglia and M. D. Pritt, *Two-Dimensional Phase Unwrapping: Theory, Algorithm, and Software* (Wiley, 1998).
2. H. A. Aebischer and S. Waldner, "A simple and effective method for filtering speckle-interferometric phase fringe patterns," Opt. Commun. **162**, 205–210 (1999).
3. K. Qian, W. Gao, and H. Wang, "Windowed Fourier-filtered and quality-guided phase-unwrapping algorithm," Appl. Opt. **47**, 5420–5428 (2008).
4. T. J. Flynn, "Consistent 2-D phase unwrapping guided by a quality map," in *Proceedings of IEEE Conference on Geoscience and Remote Sensing Symposium* (IEEE, 1996), pp. 2057–2059.
5. T. J. Flynn, "Two-dimensional phase unwrapping with minimum weighted discontinuity," J. Opt. Soc. Am. A **14**, 2692–2701 (1997).
6. W. Xu and I. Cumming, "A region-growing algorithm for InSAR phase unwrapping," IEEE Trans. Geosci. Remote Sensing **37**, 124–134 (1999).
7. M. A. Herráez, D. R. Burton, M. J. Lalor, and M. A. Gdeisat, "Fast two-dimensional phase-unwrapping algorithm based on sorting by reliability following a noncontinuous path," Appl. Opt. **41**, 7437–7444 (2002).
8. J. Bioucas-Dias and G. Valadão, "Phase unwrapping via graph cuts," IEEE Trans. Image Process. **16**, 698–709 (2007).
9. L. Meng, S. Fang, P. Yang, and L. Wang, "Quality-guided phase unwrapping algorithm based on reliability evaluation," Appl. Opt. **50**, 1925–1932 (2011).
10. M. Servin, F. J. Cuevas, D. Malacara, J. L. Marroguin, and R. Rodriguez-Vera, "Phase unwrapping through demodulation by use of the regularized phase-tracking technique," Appl. Opt. **38**, 1934–1941 (1999).
11. H. Y. Yun, C. K. Hong, and S. W. Chang, "Least-square phase estimation with multiple parameters in phase-shifting electronic speckle pattern interferometry," J. Opt. Soc. Am. A **20**, 240–247 (2003).
12. K. Qian, S. H. Soon, and A. Asundi, "A simple phase unwrapping approach based on filtering by windowed Fourier transform," Opt. Laser Technol. **37**, 458–462 (2005).
13. J. Bioucas-Dias, V. Katkovnik, J. Astola, and K. Egiazarian, "Absolute phase estimation: adaptive local denoising and global unwrapping," Appl. Opt. **47**, 5358–5369 (2008).
14. S. Fang, A. Kubo, H. Fujio, K. Oyama, Y. Saitoh, and M. Suzuki, "Digital phase data processing method for laser interferometry measurement of gear tooth flank," in *Proceedings of VDI International Conference on Gears*, Vol. 1230 (VDI-Verlag, 1996), pp. 1111–1123.
15. S. Fang, L. Wang, M. Komori, and A. Kubo, "Simulation method for interference fringe patterns in measuring gear tooth flanks by laser interferometry," Appl. Opt. **49**, 6409–6415 (2010).
16. S. Fang, L. Wang, M. Komori, and A. Kubo, "Design of laser interferometric system for measurement of gear tooth flank," Optik **122**, 1301–1304 (2011).
17. S. Fang, L. Wang, P. Yang, L. Meng, M. Komori, and A. Kubo, "Improvement of the oblique-incidence optical interferometric system to measure tooth flanks of involute helical gears," J. Opt. Soc. Am. A **28**, 590–595 (2011).
18. X. Su and W. Chen, "Reliability-guided phase unwrapping algorithm: a review," Opt. Lasers Eng. **42**, 245–261 (2004).
19. S. Esedoglu and J. Shen, "Digital inpainting based on the Mumford–Shah–Euler image model," Eur. J. Appl. Math. **13**, 353–370 (2002).
20. T. F. Chan and J. Shen, "Non-texture inpainting by curvature-driven diffusions," J. Visual Commun. Image Rep. **4**, 436–449 (2001).
21. T. F. Chan, S. H. Kang, and J. H. Shen, "Euler's elastica and curvature based inpainting," SIAM J. Appl. Math. **63**, 564–592 (2002).
22. A. Efros and W. T. Freeman, "Image quilting for texture synthesis and transfer," in *Proceedings of the 28th Annual Conference on Computer Graphics and Interactive Techniques* (ASSOC Computing Machinery, 2001), pp. 341–346.
23. I. Drori, D. Cohen-Or, and H. Yeshurun, "Fragment based image completion," ACM Trans. Graph. **22**, 303–312 (2003).
24. A. Criminisi, P. Perez, and K. Toyama, "Object removal by exemplar-based inpainting," in *Proceedings of IEEE Conference on Computer Vision and Pattern Recognition* (IEEE, 2003), pp. 1–8.
25. A. Criminisi, P. Perez, and K. Toyama, "Region filling and object removal by exemplar-based image inpainting," IEEE Trans. Image Process. **13**, 1200–1212 (2004).